Design and Analysis of a Pole-Changing Machine With Multi-Auxiliary-Teeth Structure

Wenjie Wu, Mingyuan Jiang, and Shuangxia Niu

Department of Electrical and Electronic Engineering, The Hong Kong Polytechnic University, Hong Kong 999077, China

This article proposes a multi-auxiliary-teeth pole-changing machine based on zero-sequence current. Through changing the direction of the zero-sequence current, the excitation flux field is varied and weakened to improve its flux-weakening ability. For this proposed machine, its torque and flux-weakening ability are closely related to the number of the auxiliary teeth. In this article, the performance about the multi-auxiliary-teeth structure is analyzed based on flux modulation theory in detail. Moreover, the proposed machines with the different auxiliary teeth are simulated by finite element analysis (FEA) method and further compared. According to the comparison results, the best scheme is determined with the relatively high torque and flux-weakening ability simultaneously.

***Index Terms*— Flux-weakening capability, multi-auxiliary-teeth, pole-changing machine, zero-sequence current.**

I. Introduction

DUE to the multiple advantages of low maintenance cost and high efficiency, the direct-drive permanent magnet (PM) machines have many potentials in actual applications [1], [2], [3], [4], [5]. For the direct drive machine, the requirement of the torque density is higher than other conventional machines. As the representative machine with high torque density, the PM flux modulation machine has attracted the considerable attention because of the flux modulation effect [5], [6], [7], [8], [9], [10], [11], [12]. In order to reduce the usage of PMs and further decrease the cost of the flux modulation machine, the zero-sequence current is injected in the PM flux modulation machines [13]. The injected zero-sequence current can be served as the additional excitation source to generate the excitation flux field, which means that some part of the PMs can be replaced.

Apart from the torque density, the rotating speed range is also the important performance for the practical application of this type of machine. The key to present a wider range of rotational speeds is to improve the flux-weakening ability. i_d current represents the d-axis current. Due to the fixed shape of PMs, the traditional flux-weakening method is to inject i_d current to weaken the armature flux field. However, the injected i_d current makes the negative effect on the copper loss and efficiency without increasing the torque density. In order to improve flux-weakening ability and maintain the high efficiency simultaneously, the new concept "pole changing" is proposed.

With the help of the pole-changing operation, the pole-pair number can be changed, resulting in the variation of the flux field. Pole-changing operation is widely used in PM flux modulation machines through the additional structural modifications or controller circuits. In order to realize the more convenient and concise pole-changing operation, a novel pole-changing machine based on zero-sequence current is proposed in this article. The injected zero-sequence current can generate the additional excitation flux field to reduce PM usage and achieve the pole-changing effect through reversing its direction.

Based on the pole-changing operation, the flux-weakening ability is enhanced and expand the rotating speed range.

For this proposed pole-changing machine, the number of multi-auxiliary-teeth has the intimate relationship with the torque performance and flux-weakening ability. It is because it is related to the variation multiples of the excitation source pole-pair number during pole-changing operation. It means that it affects the flux field of the proposed machine when performing pole-changing operation.

In order to reveal the specific connection between torque density, flux-weakening ability, and multi-auxiliary-teeth number, their formulas are built and analyzed in this article according to the flux modulation principle and pole-changing principle. Moreover, the different four schemes are proposed and simulated through finite element analysis (FEA) method based on the different auxiliary teeth to verify the effectiveness of the flux-weakening ability improvement during pole-changing operation. With the help of the comparison results, the scheme with the most reasonable multi-auxiliary-teeth structure is selected due to the relatively high torque density and improved flux-weakening ability simultaneously.

The rest of this article is arranged as follows. In Section II, the machine configuration is introduced together with the working principle and pole-changing mechanism. In Section III, the different four schemes with the different stator auxiliary teeth are compared based on the simulated results. Finally, the best optimal scheme is selected through the comparison result. The conclusion component is summarized in Section IV.

II. Machine Configuration and Operating Principle

A. Machine Configuration

For the sake of realizing the flux-weakening ability enhancement and speed range expansion based on pole-changing

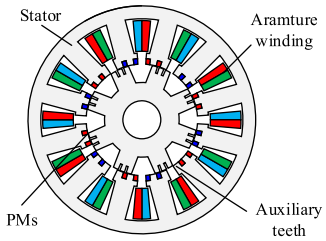

Fig. 1. Proposed structure of pole-changing machine.

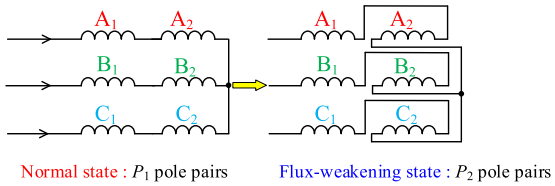

Fig. 2. Basic principle of IW.

operation, an 8-tooth/12-slot pole-changing machine with the multi-auxiliary-teeth structure, which is shown in Fig. 1, is selected to verify its effectiveness. From Fig. 1, it is shown that the PMs are installed on the stator. These parts, together with the injected zero-sequence current, constitute the excitation source of the proposed machine. When the polarity of the PMs is fixed, the variation of the zero-sequence current direction means that the pole-pair number of the whole excitation source is changed to weaken excitation flux field. The pole-pair number of excitation source generated by zero sequence current is consistent with the number of auxiliary teeth, which affects the varied flux field during pole-changing operation.

Moreover, the pole-changing operation will introduce more harmonics to increase the torque ripple of the proposed machine. Therefore, the notching teeth are designed on rotor to suppress the torque ripple.

B. Excitation Flux Field Analysis

By multiplying the air-gap magnetomotive force (MMF) and permeance, the air-gap flux density is achieved, which can be shown as

$$\begin{aligned} B(\theta,t) &= F(\theta)\times\Lambda_r(\theta,t)\\ &= C_1\Lambda_{r0}\cos(N_e\theta)\\ &\quad+\frac{1}{2}C_1\Lambda_{r1}\cos[(N_e+N_r)\theta-N_r\Omega_{r1}t]\\ &\quad+\frac{1}{2}C_1\Lambda_{r1}\cos[(N_e-N_r)\theta+N_r\Omega_{r1}t] \end{aligned} \tag{1}$$

where N_e is the pole-pair numbers of the excitation sources, N_r is the number of rotor salient poles, Λ_r represents the air-gap permeance generated by stator teeth and rotor teeth, respectively, Ω_r is the mechanical angular speed, and C is the amplitude of the air-gap harmonic.

Through integrating the flux density, the flux linkage generated by PM and dc excitation sources is achieved, which is shown as follows:

$$\begin{aligned} \varphi(t) &= r_g l_{\text{ef}} n_c \int_{-\pi * y_{\text{ph}}/N_s}^{\pi * y_{\text{ph}}/N_s} B(\theta,t)d\theta\\ &= C_1\Lambda_{r0}\frac{2r_g l_{\text{ef}} n_c}{N_e}\sin\frac{\pi y_{\text{ph}} N_e}{N_s}\cos N_r\Omega_r t\\ &\quad+\frac{C_1\Lambda_{r1}}{2}\frac{2r_g l_{\text{ef}} n_c}{N_e\pm N_r}\sin\frac{\pi y_{\text{ph}}(N_e\pm N_r)}{N_s}\cos N_r\Omega_r t \end{aligned} \tag{2}$$

where r_g is the air-gap radius, l_{eg} is the axial length, n_c is the winding turns, y_{ph} is the corresponding coil pitch, and N_s represents the number of the stator slots.

Furthermore, the back electromotive force (back EMF) equation can be expressed as follows:

$$E = 4.44k_n N f_d \varphi \tag{3}$$

where k_n is the winding factor and f_d is the frequency of the proposed machine.

The improvement of flux-weakening ability means the reduction of the back EMF amplitude. Under the same constraint of the maximum bus voltage, the lower back EMF means the smaller q-axis current. Moreover, the q-axis current and maximum speed $\omega_{\max}$ satisfy the following relationship:

$$I_q = \frac{u_{\max}}{\omega_{\max} L_q}. \tag{4}$$

Because of the lower q-axis current, maximum rotating speed $\omega_{\max}$ in flux-weakening state is larger than that in the normal state, thereby achieving the speed expansion effect.

According to (2) and (3), it can be found that the flux linkage and back EMF are determined by (N_e)th harmonic components generated by dc and PM excitation sources and $|N_e \pm N_r|$th harmonic component modulated by modulation tooth structure.

With the help of the pole-changing operation, the pole-pair numbers of the excitation sources are transformed into multiple times larger than original one. Therefore, the pole-pair number of the excitation sources is equal to nN_e in flux-weakening state when completing the pole-changing operation. Its multiple time is equal to the number of the auxiliary teeth, which is shown in Fig. 2. Fig. 2 shows the specific stator tooth structures corresponding to different auxiliary teeth in the four proposed schemes. The multiple time n is equal to 1, 2, 3, and 4 for the four different schemes, respectively.

The difference value of the back EMF during pole-changing operation can represent the flux-weakening ability of the proposed machine, which can be expressed as follows:

$$\begin{aligned} D_b &= E_2 - E_1 = 4.44k_n N f_d(\varphi_2-\varphi_1)\\ &= C_1\Lambda_{r0}\left(\frac{2r_g l_{\text{ef}} n_c}{nN_e}\sin\frac{\pi y_{\text{ph}} nN_e}{N_s}\right.\\ &\qquad\left.-\frac{2r_g l_{\text{ef}} n_c}{N_e}\sin\frac{\pi y_{\text{ph}} N_e}{N_s}\right)\cos N_r\Omega_r t\\ &\quad+\frac{C_1\Lambda_{r1}}{2}\left(\frac{2r_g l_{\text{ef}} n_c}{nN_e\pm N_r}\sin\frac{\pi y_{\text{ph}}(nN_e\pm N_r)}{N_s}\right.\\ &\qquad\left.-\frac{2r_g l_{\text{ef}} n_c}{nN_e\pm N_r}\sin\frac{\pi y_{\text{ph}}(nN_e\pm N_r)}{N_s}\right)\cos N_r\Omega_r t. \end{aligned} \tag{5}$$

From (4) and (5), it can be seen that the back EMF and flux-weakening ability are both closely related to the auxiliary teeth number n, respectively. As the number of auxiliary teeth increases, the back EMF of the proposed machine will increase, while the flux-weakening ability will decrease. Besides, the auxiliary teeth number also influences the structural complexity of the proposed machine. Therefore, it is necessary to choose the reasonable auxiliary teeth number considering the torque and flux-weakening ability simultaneously through subsequent simulation analysis.

C. Integrated Winding

In order to simplify the winding structure and increase the effective slot area of the machine, thereby increasing the torque density, the integrated winding (IW) [14], [15] is applied in the proposed machine. The function of the IW is to achieve the different winding configurations on the same set of windings through the selection of specific winding pole pairs, as shown in Fig. 2. With the help of the IW, the original air-gap flux field can be transformed to another air-gap flux field with the different winding arrangements. Its design can be adopted to weaken the air-gap flux field, thus improving the flux-weakening capability.

The modulated harmonic orders require to match with the winding pole-pair number during pole-changing operation. Therefore, the winding pole-pair numbers P_1 and P_2 during the pole-changing operation need to meet the formula as follows:

$$\begin{cases} |N_e \pm N_r| = |P_1 \pm iN_s| \\ |nN_e \pm N_r| = |P_2 \pm iN_s| \end{cases} \tag{6}$$

where n is equal to the number of excitation sources on a single stator tooth.

Moreover, the IW structure has the specific requirement about the winding pole-pair numbers. Therefore, the IW pole-pair numbers P_1 and P_2 in this article require to meet the following relationships:

$$\mathrm{GCD}(N_s, P_1) = \frac{1}{2}\mathrm{GCD}(N_s, P_2) \tag{7}$$

where GCD is the greatest common divisor.

For the selected 8-tooth/12-slot pole-changing machine in this article, N_e, N_s, and N_r are equal to 6, 12, and 8, respectively. When the auxiliary teeth number n is equal to 1, 2, 3, and 4 in four proposed different schemes, the relationships in (6) and (7) are satisfied. Therefore, these four schemes with the different auxiliary teeth number, which are illustrated in Fig. 3, are selected to make the comparison and conduct the subsequent simulation.

III. Proposed Machine Simulation and Comparison

To ensure fairness in comparative simulation, the usage of PMs for different schemes maintains the consistent level. Therefore, the widths of PMs w_{pm} and auxiliary teeth w_a are designed with the different values. Besides, the other parameters remain unchanged. Table I shows the main parameters of four different schemes.

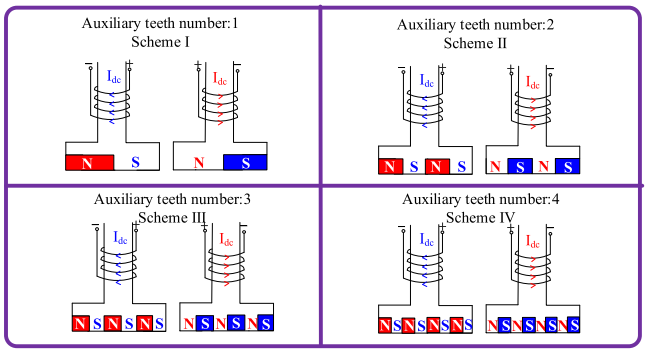

Fig. 3. Proposed different four schemes based on the different auxiliary teeth numbers.

TABLE I
Design Parameters of Pole-Changing Machines

Items	n=1	n=2	n=3	n=4
Stator slot number	12			
Rotor tooth number	8			
Excitation source pole-pair number	12	24	36	48
Width of auxiliary teeth w_a (deg)	20	10	5	2.5
Width of rotor teeth w_1 (deg)	20			
Height of stator teeth h_{a1} (mm)	18			
Height of rotor teeth h_{a2} (mm)	9.3			
Width of PMs w_{pm} (deg)	8	4	2	1
Height of PMs h_{pm} (mm)	3			

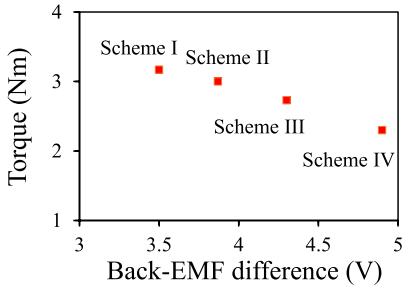

Fig. 4. Comparison of the torque and flux-weakening performance between the four different schemes.

To compare the torque performance and flux-weakening ability of the four different schemes, the back EMF and torque waveforms are simulated in Section III. Fig. 4 shows the comparison results of those four schemes. The back EMF difference represents the flux-weakening ability of the four proposed schemes. When the difference values are larger, the pole-changing effect and speed range expansion are better. Therefore, from Fig. 4, it can be seen that the flux-weakening ability is improved as the number of auxiliary teeth increases. On the contrary, the torque performance becomes worse along with the increase the auxiliary teeth number. Moreover, the average torque values of schemes I and II are approximately close. This is mainly due to the reason that scheme I did not achieve optimal saturation at the same current condition. Fig. 5 shows the flux density distribution of schemes I and II. It is illustrated that the flux density of the auxiliary teeth in scheme II is much closer to 2T, which means that its saturation condition is better than scheme I with the same dc excitation current. Therefore, with regard to the two performances of

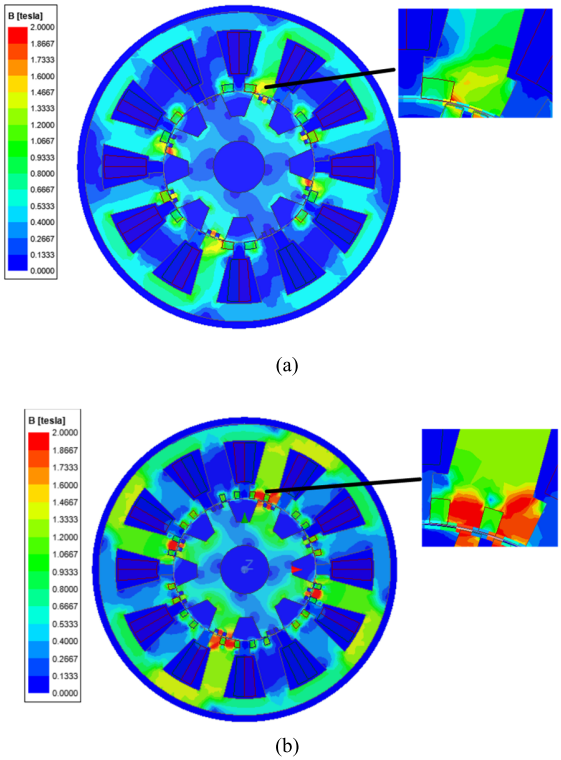

Fig. 5. Air-gap flux density distribution. (a) Scheme I. (b) Scheme II.

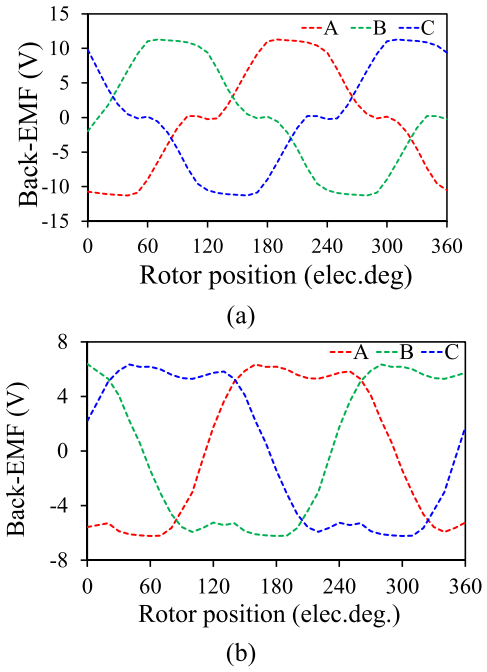

Fig. 6. Back EMF waveforms of scheme IV in different operating states. (a) Normal state. (b) Flux-weakening state.

torque and flux-weakening ability, schemes II and IV are selected for further comparison.

Fig. 6(a) and (b) illustrates the back EMF waveforms of the proposed scheme IV in the normal and flux-weakening states, respectively. From Fig. 6(a) and (b), it can be observed that the waveforms of the back-EMFs are not absolutely sinusoidal. Due to the relatively large number of stator auxiliary teeth,

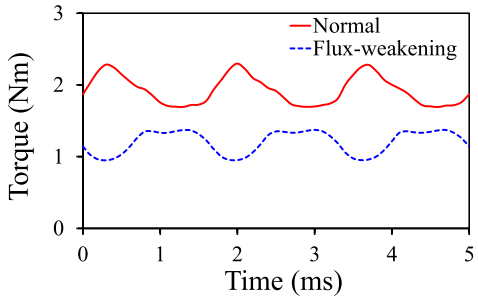

Fig. 7. Waveforms of the torque in normal and flux-weakening states for scheme IV.

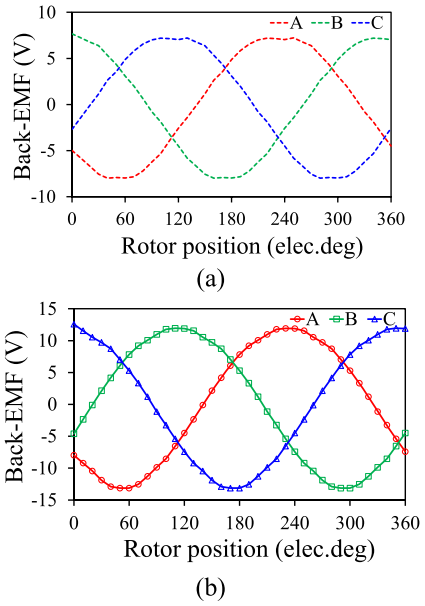

Fig. 8. Back EMF waveforms of scheme II in different operating states. (a) Normal state. (b) Flux-weakening state.

the back EMF of scheme IV has more harmonics. Fig. 7 shows the torque waveforms in normal and flux-weakening states. It can be seen that the torque ripple has relatively large values because of the negative influence of the more harmonics. Considering the greater difficulty in manufacturing the tooth structure of this scheme, although it has good torque and flux-weakening performance, it also has many defects.

Fig. 8(a) and (b) presents the back EMF waveforms of the proposed scheme IV in the normal and flux-weakening states, respectively. It is shown that the amplitudes of the back EMF decrease from 14.2 to 8.5 V during pole-changing operation, both with nearly 40% reduction. It means that the proposed scheme II can exhibit the excellent flux-weakening improvement during pole-changing principle.

Fig. 9 shows the torque waveforms of the proposed scheme II. It can be seen the average torque value in normal state is about 2.8 N·m, which coincides with the results in Fig. 4. With the help of the pole-changing operation, the average torque value in flux-weakening state is close to 1.8 N·m. Moreover, the torque ripples in the normal and flux-weakening states are both lower than 15%. Due to the low harmonic content included in this scheme, the torque ripples before and after pole-changing operation are both not significant. Therefore,

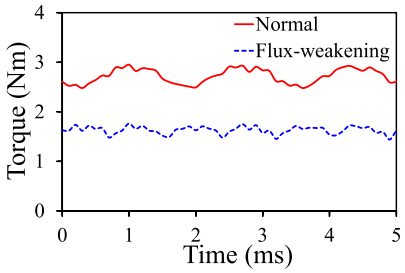

Fig. 9. Waveforms of the torque in normal and flux-weakening states for scheme II.

based on the above comparison results, when the number of stator auxiliary teeth is equal to 2, the comprehensive performance of this scheme has the more advantages.

IV. Conclusion

In this article, a multi-auxiliary-teeth pole-changing machine based on zero-sequence current is proposed to improve the flux-weakening ability. The number of auxiliary teeth has a significant impact on the torque and flux-weakening ability of the proposed machine. First, the specific impact is theoretically analyzed based on flux field modulation theory, machine structure, and pole-changing principle. Moreover, the different four schemes are proposed and compared. Through comprehensive comparison of torque, flux-weakening ability, torque ripple, saturation performance, and other aspects, the scheme with the two auxiliary teeth is selected the optimal best solution. Finally, the electromagnetic back EMF and torque performance of the scheme with the two auxiliary teeth is analyzed and simulated to verify its effectiveness.

Acknowledgment

This work was supported in part by the National Natural Science Foundation of China under Project 52077187; and in part by the Research Grant Council, Hong Kong, China, under Project Polyu 152109/20E.

References

[1] L. Xu, G. Liu, W. Zhao, X. Yang, and R. Cheng, "Hybrid stator design of fault-tolerant permanent-magnet Vernier machines for direct-drive applications," *IEEE Trans. Ind. Electron.*, vol. 64, no. 1, pp. 179–190, Jan. 2017.

[2] Z. Li and S. Niu, "A double-sided complementary Vernier PM linear machine with high magnet utilization factor using third-order harmonics," *IEEE Trans. Ind. Electron.*, vol. 71, no. 9, pp. 11217–11228, Sep. 2024.

[3] C. Gong and F. Deng, "Design and optimization of a high-torque-density low-torque-ripple Vernier machine using ferrite magnets for direct-drive applications," *IEEE Trans. Ind. Electron.*, vol. 69, no. 6, pp. 5421–5431, Jun. 2022.

[4] Y. Shen, T. Shi, Q. Lu, and C. Xia, "Robust design and analysis of asymmetric-excited flux reversal PM linear machine for long-stroke direct drive propulsion," *IEEE Trans. Magn.*, vol. 57, no. 6, pp. 1–4, Jun. 2021.

[5] X. Zhao, S. Niu, X. Zhang, and W. Fu, "Flux-modulated relieving-DC-saturation hybrid reluctance machine with synthetic slot-PM excitation for electric vehicle in-wheel propulsion," *IEEE Trans. Ind. Electron.*, vol. 68, no. 7, pp. 6075–6086, Jul. 2021.

[6] Y. Ma, S. Niu, W. Fu, and J. Fei, "A direct-drive rotary-linear machine with dual-PM flux modulation for 2-DOF kinematic device," *IEEE Trans. Transport Electrific.*, vol. 11, no. 1, pp. 4296–4312, Feb. 2025, doi: 10.1109/TTE.2024.3458969.

[7] J. Jiang, S. Niu, and X. Zhang, "Torque improvement of a hybrid-excited Vernier reluctance machine with high-order-harmonic winding design for electric vehicle application," *IEEE Trans. Transport Electrific.*, vol. 10, no. 2, pp. 2397–2407, Jun. 2024.

[8] Y. Bi, W. Fu, S. Niu, X. Zhao, and J. Huang, "Design of a dual-set permanent magnet flux-switching machine with enhanced torque density and fault-tolerance capability," *IEEE Trans. Transport Electrific.*, vol. 10, no. 4, pp. 9096–9108, Dec. 2024, doi: 10.1109/TTE.2023.3346820.

[9] R. Wang, B. Wang, H. Cai, M. Cheng, and W. Hua, "Research on the magnetic field modulation effect of pmvm from the perspective of armature magnetic field," *IEEE Trans. Ind. Electron.*, early access, Sep. 19, 2024, doi: 10.1109/TIE.2024.3454352.

[10] S. Wang, J. Zhang, N. Wang, and Y. Wu, "Investigation of dual-sided consequent-pole flux-modulated permanent-magnet machine by air-gap field modulation theory," *IEEE Trans. Magn.*, vol. 60, no. 12, pp. 1–5, Dec. 2024, doi: 10.1109/TMAG.2024.3459048.

[11] Q. Wang, S. Niu, S. L. Ho, W. Fu, and S. Zuo, "Design and analysis of novel magnetic flux-modulated mnemonic machines," *IET Electric Power Appl.*, vol. 9, no. 7, pp. 469–477, Aug. 2015.

[12] T. Sheng, S. Niu, and S. Yang, "A novel design method for the electrical machines with biased DC excitation flux linkage," *IEEE Trans. Magn.*, vol. 53, no. 6, pp. 1–4, Jun. 2017, doi: 10.1109/TMAG.2017.2661989.

[13] S. Jia, Y. Liang, D. Liang, and J. Liu, "A novel DC-biased phase current-independent drive high-speed Vernier reluctance machine," *IEEE Trans. Magn.*, vol. 57, no. 6, pp. 1–5, Jun. 2021, doi: 10.1109/TMAG.2021.3064023.

[14] X. Ren, D. Li, R. Qu, X. Han, and Z. Liang, "A brushless dual-electrical-port dual-mechanical-port machine with integrated winding configuration," *IEEE Trans. Ind. Electron.*, vol. 68, no. 4, pp. 3022–3032, Apr. 2021.

[15] Z. Liang, X. Ren, D. Li, and R. Qu, "Analysis of integrated winding configuration in dual-electrical-port machine," *IEEE J. Emerg. Sel. Topics Power Electron.*, vol. 10, no. 2, pp. 1891–1901, Apr. 2022.